

Shear-Induced Degradation of Linear Polyacrylamide Solutions during Pre-Electrophoretic Loading

Maribel Vazquez,[†] Dieter Schmalzing,[†] Paul Matsudaira,[†] Daniel Ehrlich,[†] and Gareth McKinley^{*,†}

Whitehead Institute for Biomedical Research, 9 Cambridge Center, Cambridge, Massachusetts 02142, and Department of Mechanical Engineering, Massachusetts Institute of Technology, 77 Massachusetts Avenue, Room 3-250 Cambridge, Massachusetts 02139

Electrophoretic channels are filled with a polymer matrix prior to their use in DNA separations. This process, called gel-loading, can be accomplished manually, using syringes, or can be automated through the use of small pumps or vacuum. The injection rate is constrained by the desire to minimize shear-induced degradation of the polymer molecules. Currently, the community lacks quantitative data with which to gauge the range of flow rates that prevent polymer degradation. In this study, measurements of the zero shear rate viscosity of linear polyacrylamide (LPA) solutions are used to determine the LPA molecular weight before and after gel-loading. The results indicate molecular degradation in polymer solutions even when injected at minimal flow rates of 1 $\mu\text{L}/\text{min}$. To correlate these rheological observations of shear-induced degradation with subsequent electrophoretic performance, the degraded solutions were used as sieving matrixes for DNA sequencing analysis. The decreases in electrophoretic resolution and increases in peak widths between sheared and nonsheared LPA solutions are related to the degradation in molecular weight experienced by the polymer solutions.

Entangled solutions of linear polyacrylamide (LPA) are widely used in electrophoresis, performed in both capillaries and micro-fabricated devices, because of their excellent sieving capacity during DNA separations.^{1–3} Researchers typically use solutions of unbranched LPA with an average molecular mass of 9–13 MDa and concentrations between 2 and 6 wt % (w/v).⁴ The highly entangled polymer matrix is gel-like with “pores” between the entanglement points that provide the necessary sieving for DNA separations by molecular size.⁵ Video microscopy studies have illustrated how entangled polymer chains of the matrix are actively

dragged by DNA molecules during electrophoretic separations.^{6,7} Consequently, the level of chain entanglement in the polymer solution, pore structure, and monomer length play a significant role in the mechanism and quality of electrophoretic DNA separations.^{4,8,9}

Currently, there is no standard protocol by which LPA solutions are loaded into electrophoretic channels. Filling may be accomplished manually, through the use of syringes,¹⁰ and may incorporate automated pumps^{11,12} or the use of vacuum. With any method of filling, however, the narrow gaps of electrophoretic channels produce high shear rates along the channel walls during gel-loading.¹³ Such shear rates can affect the strand length and entanglement density of polymer solutions via chain scission or coil disentanglement. Since the LPA matrix creates a network in which DNA molecules are sieved, any distortion or rupture of the polymer chains, and/or their configuration, affects DNA migration within the channel. Molecular degradation of LPA solutions is, therefore, of great practical interest because any change in DNA navigation affects subsequent sequencing analysis. Such shear-induced changes in the viscoelastic properties of an entangled solution can be monitored by rheological observation. For a complete theoretical review, the reader is referred to the texts of Doi and Edwards¹⁴ and Bird, Armstrong, and Hassager.¹⁵

Rheology provides a means to extract molecular information about polymer solutions from bulk measurements of the fluid viscoelasticity. Previous work with dilute and concentrated solutions has illustrated how the zero shear rate viscosity of a polymer matrix, η_0 , can be used to identify its molecular weight.¹⁶ For dilute

* To whom correspondence should be addressed: (e-mail) gareth@mit.edu; (phone) (617)258-0754; (fax) (617)258-8559.

[†] Whitehead Institute for Biomedical Research.

[‡] Massachusetts Institute of Technology.

- (1) Heiger, D. N.; Cohen, A. S.; Karger, B. L. *J. Chromatogr.* **1990**, *516*, 33–48.
- (2) Cohen, A. S.; Najarian, D. R.; Karger, B. L. *J. Chromatogr.* **1990**, *526*, 49–60.
- (3) Sunada, W. M.; Blanch, H. W. *Electrophoresis* **1997**, *18*, 2243–2254.
- (4) Carrilho, E.; Ruiz-Martinez, M. C.; Berka, J.; Smirnov, I.; Goetzinger, W.; Miller, A. W.; Brady, D.; Karger, B. L. *Anal. Chem.* **1996**, *68*, 3305–3313.

- (5) Wu, C.; Quesada, M. A.; Schneider, D. K.; Farinato, R.; Studier, F. W.; Chu, B. *Electrophoresis* **1996**, *17*, 1103–1109.
- (6) Mitnik, L.; Salone, L.; Viovy, J. L.; Heller, C. *J. Chromatogr., A* **1995**, *710*, 309–321.
- (7) Carlsson, C.; Larsson, A. In *Analysis of Nucleic Acids by Capillary Electrophoresis*; Heller, C., Ed.; Vieweg: Wiesbaden, Germany, 1997; pp 67–89.
- (8) Heller, C. *Electrophoresis* **1999**, *20*, 1978–1986.
- (9) Heller, C. *Electrophoresis* **1999**, *20*, 1962–1977.
- (10) Schmalzing D.; Adourian A.; Koutny L.; Ziaugra L.; Matsudaira P.; Ehrlich D. *Anal. Chem.* **1998**, *70*, 2303–2310.
- (11) PE Applied Bio Systems. *1998 Automated DNA Sequencing/ABI Prism 310 User's Manual*; Foster City, CA, 1998.
- (12) Molecular Dynamics *MegaBase 1000 Training*; Sunnyvale, CA, 1999.
- (13) Fay, J. A. *Introduction to Fluid Mechanics*; MIT Press: Cambridge MA, 1994.
- (14) Doi, M.; Edwards, S. F. *The Theory of Polymer Dynamics*; Oxford University Press: Oxford, U.K., 1986.
- (15) Bird, R. B.; Armstrong, R. C.; Hassager, O. *Dynamics of Polymeric Liquids*; John Wiley and Sons: New York, 1987.

systems, the zero shear rate viscosity is related to the intrinsic viscosity by a Taylor series expansion.¹⁵

$$\eta_0/\eta_s = \eta_s[1 + [\eta]c + K[\eta]^2c^2 + \dots] \quad (1)$$

where $[\eta]$ is the intrinsic viscosity, or limiting viscosity number¹⁷ (in units of mL/g), η_s is the solvent viscosity, c is concentration (in mL/g), and K is the Huggins coefficient¹⁶ specific to a given polymer–solvent pair. The intrinsic viscosity can be obtained experimentally using an Ostwald viscometer and is a rheological measure of how a fluid's viscosity increases with its molecular weight. Note, Equation 1 is only appropriate to determine the zero shear rate viscosity, η_0 , for dilute solutions in which $c[\eta] < 1$.^{18–21} For entangled materials, rheological measurements and theoretical analysis shows that the zero shear rate viscosity is proportional to the viscosity-averaged molecular weight, M_v , to approximately the 3.4 power.¹⁵

$$\eta_0 \sim M_v^{3.4} \quad (2)$$

Viscometric data are, thus, a very sensitive probe of small changes in the molecular weight of an entangled polymer solution. The molecular weight of a polymer solution provides an estimate for the pore structure and chain disentanglement of the polymer matrix. In particular, the number of entanglement points is given by

$$N_e = M/M_e \quad (3)$$

where M_e is the entanglement molecular weight, defined as the molecular weight between entanglement points.¹⁴ This value is $\sim 10^5$ for an LPA concentration of 11%.²² Since electrophoresis depends on the number and size of pores between entanglement points,⁹ monitoring changes in polymer molecular weight can determine changes to these parameters. In the present study, we relate the zero shear rate viscosity, η_0 , to the molecular weight through experimental calibration, as will be described in the Materials and Methods section.

The current study describes experiments performed using an automated syringe pump for gel-loading. Here, 2 and 3% (w/v) concentrations of unbranched LPA solutions, of 9×10^6 molecular weight dissolved in water, were loaded into 12-cm-long capillaries of 50- and 75- μm internal diameters. Given these dimensions, the polymer volume within a filled capillary is 0.23 and 0.53 μL , respectively. The polymer matrixes were loaded into the channels at measured fill times between 1 s and 2 min. It is useful to convert each fill time into an average volume flow rate, Q . An imposed flow rate of 1 $\mu\text{L}/\text{min}$, for example, means that the polymer volume

within a 12-cm-long-capillary is replaced twice per minute. Although flow rates used during gel-loading are generally not reported in the literature, using a timer, we estimated that reasonable fill times for a 12-cm-long channel lie between 30 and 90 s, corresponding to a flow rate of $\sim 15 \mu\text{L}/\text{min}$. For completeness, rheology data for flow rates ranging between 1 and 33 $\mu\text{L}/\text{min}$ will be discussed.

The tests in the present work quantify polymer degradation by relating the zero shear rate viscosity, η_0 , to the viscosity-averaged molecular weight, M_v , before and after gel-loading. Molecular weight averaging is needed for polydisperse solutions since typical samples of linear macromolecules have a distribution of molecular weights as a consequence of their chemical synthesis. Unlike the more conventional number-averaged molecular weight, M_n , and weight-averaged molecular weight, M_w , the viscosity-averaged molecular weight, M_v , is a polynomial average related to the hydrodynamic volume of the chain.

$$M_v = \left(\sum w_i M_i^a / \sum w_i \right)^{1/a} \quad (4)$$

where w_i is the fraction of strands of degree of polymerization i , M_i is the individual molecular weight of a polymer strand i , and a is the polymer-specific exponent from the Mark–Houwink–Sakurada equation.²³ The heterogeneity index, (M_w/M_n) , is often used as a measure of the polydispersity of a solution. Equation 4 is valid for polymer solutions with $(M_w/M_n) < 3$ and peak molecular weights between 10^2 and 10^8 .²³ The LPA solutions used in this study fall within these limits with heterogeneity index $(M_w/M_n) < 2$ and peak molecular weights of order 10^7 .²²

The viscometric properties of each collected polymer sample were measured using a cone and plate rheometer. To correlate the rheological results to DNA sequencing analysis, LPA solutions in which degradation was identified were used as separation matrixes during electrophoresis performed on 12-cm-long micro-fabricated channels. The increases in peak widths and decreases in electrophoretic resolution between the degraded and nondegraded LPA solutions are correlated to the decrease in molecular weight as a result of shear-induced degradation.

THEORY

Shear Rates. LPA solutions used for electrophoretic DNA separations are typically entangled solutions, where individual molecules interpenetrate forming entanglements. In a basic polymer system, macromolecules are separated by large distances that minimize individual interactions between the molecules. In more complex systems, macromolecules are highly entangled and interact with one another so strongly that the contributions of individual macromolecules are hard to distinguish.²⁴ At low polymer concentrations, solution properties are determined by the properties of individual macromolecules and the solutions are classified as dilute. With increasing concentration, polymer coils begin to overlap forming semidilute, and eventually concentrated, solutions.

A parameter called the overlap threshold, or critical concentration, c^* , denotes the region where polymer molecules just begin

(16) Brandup, I. *Polymer Handbook*, 3rd ed.; John Wiley and Sons: New York, 1989.

(17) Clay, J. D.; Koelling, K. W. *Polym. Eng. Sci.* **1997**, *37*, 793–805.

(18) Graessley, W. M. *Adv. Polym. Sci.* **1974**, *16*, 1–284.

(19) Duke, T.; Viovy, J. L.; Semenov, A. N. *Biopolymers* **1994**, *34*, 239–247.

(20) Hubert S. J.; Slater, G. W.; Viovy, J. L. *Macromolecules* **1996**, *29*, 1006–1009.

(21) Slater, G. W.; Kist, T. B. L.; Ren, H.; Drouin, G. *Electrophoresis* **1998**, *19*, 3133–3142.

(22) Kulicke, W. M.; Kniewske, R.; Klein, *Proc. Polym. Sci.* **1992**, *8*, 373–468.

(23) Shroder, E.; Muller, G.; Arndt, K. F. *Polymer Characterization*; Hanser Publishers: Munich, 1982.

(24) Grosberg, A. Y.; Khokhlov, A. R. *Giant Molecules: Here, and There, and Everywhere*; Academic Press: San Diego, 1997.

to interact. Solutions with concentrations greater than c^* are considered semidilute. As the polymer coils continue to overlap and interpenetrate, a new parameter called the entanglement concentration, c^\dagger , defines the region of concentrated solutions.²⁶ Scaling arguments show that the entanglement concentration, c^\dagger , is independent of molecular weight for $M_v \geq M_e$. For LPA solutions with molecular masses within 9–13 MDa, the critical concentration, c^* has been experimentally verified as 0.1%²² while the entanglement concentration, c^\dagger , is $\sim 10\%$.^{22–26} LPA solutions of 2 and 3% (w/v) typically used for DNA separations are therefore within the semidilute, entangled regime.¹⁸

During gel-loading, LPA solutions are exposed to large shear stresses as they are forced under pressure into microfabricated channels or capillaries. The resulting effect of the shear stress depends on the types of flow that occur during LPA injection. A typical gel-loading protocol may inject LPA solutions into capillaries by using a small syringe, for example. In such an instance, LPA is ejected from a 500- μL syringe, with needle diameter 350 μm , into an electrophoretic channel of diameter 75 μm , forcing the polymer through an area contraction of 22:1. Flows through such contractions are classified as fast transient flows (FTF) and are well documented to result in polymer degradation independent of specific nozzle geometry.²⁹ Further, once inside the electrophoretic channel, the polymer solution is forced along the channel under constant pressure gradient. During this process, the solution experiences a steady shearing flow with a distribution of shear rates increasing from zero at the centerline, to a maximum at the channel walls.¹⁵ Numerous papers show that high molecular weight polymers are easily fractured in such common pure shear flows configurations.^{30–33} The shear rate imposed during this gel-loading is of the order

$$\dot{\gamma} \equiv dv_z/dr \sim Q/\pi R^3 \quad (5)$$

where Q is the volume flow rate and R is the channel radius. For the flow rates and channel sizes discussed above, shear rates in the range $10^2 \leq \dot{\gamma} \leq 10^3 \text{ s}^{-1}$ can be experienced.

Non-Newtonian Viscosity. The viscosity, η , of an entangled polymer solution is a strong function of the shear rate since the orientation of polymer segments, and the number of entanglement points in the material depends on the externally applied load. The shear rate-dependent viscosity, $\eta(\dot{\gamma})$, is a viscometric material function that can be determined using a plate and cone rheometer. In this device, the polymer solution is placed within the thin gap formed between an inverted cone and plate as the cone is rotated at different angular velocities. For small cone angles, a homogeneous shear flow develops in the gap, and by varying the imposed torque, the viscosity as a function of shear rate, $\dot{\gamma}$, or shear stress, τ , is obtained.¹⁵

(25) Grossman, P. D.; Soane, D. S. *J. Chromatogr.* **1991**, *559*, 257–266.

(26) Graessley, W. M. *Polymer* **1980**, *21*, 258–262.

(27) Bouldin, M.; Kulicke, W. M.; Kehler, H. *Colloid Polym. Sci.* **1998**, *266*, 763–805.

(28) Cottet, H.; Gareil, P.; Viovy, J. L. *Electrophoresis* **1998**, *19*, 2151–2162.

(29) Nguyen, T. Q.; Kausch, H. H. *Colloid Polym. Sci.* **1991**, *269*, 1099–1110.

(30) Kim, S.; Hobbie, E. K.; Yu, J. W.; Han, C. C. *Phys. Fluids: Plasma Biophys.* **1998**, *20*, 2301–2314.

(31) Flew, S.; Sellin, R. H. J. *J. Non-Newtonian Fluid Mech.* **1993**, *47*, 169–210.

(32) Scott, J. P.; Fawell, P. D.; Ralph, D. E.; Farrow, J. B. *J. App. Polym. Sci.* **1996**, *62*, 2097–2106.

(33) D'Almeida, A. R.; Dias, M. L. *Polym. Degrad. Stab.* **1997**, *56*, 331–337.

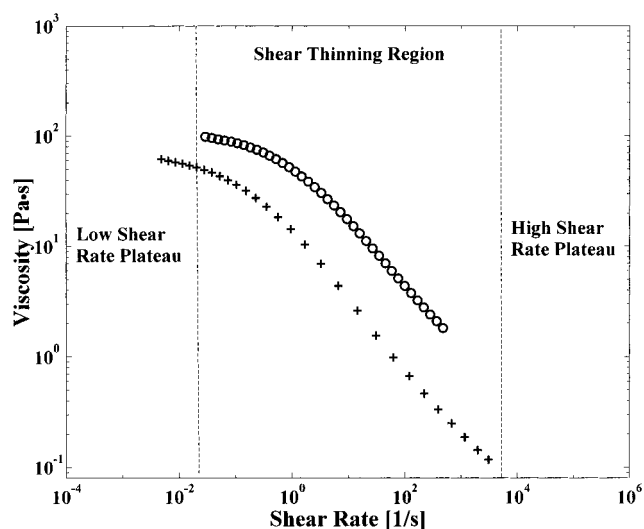


Figure 1. Characteristic non-Newtonian viscosity profiles for a 2% (w/v) LPA solution of 2.2×10^6 molecular weight. The lower curve illustrates viscometric measurements for a solution of LPA dissolved in deionized water at 25 °C, while the upper curve illustrates viscometric data for a solution of LPA dissolved in a $1 \times$ TBE separation buffer (90 mM Tris/64.6 mM boric acid/2.5 mM EDTA). The low shear rate, shear thinning, and high shear rate regions are identified. Note, data in the high shear rate region are generally unobtainable as shear rates greater than 10^4 are required.

A typical viscosity profile for a 2% LPA solution generated by a cone and plate rheometer is shown in Figure 1. The figure displays two curves, upper and lower, of an LPA solution dissolved in buffer¹⁰ and deionized water, respectively. Each curve displays experimental viscosity values for shear rates spanning 6 orders of magnitude. Typically the non-Newtonian viscosity has three characteristic regions: a low shear rate plateau, a shear thinning region, and a high shear rate plateau. The low shear rate plateau corresponds to viscosity values obtained below shear rates of $\dot{\gamma} \sim \lambda^{-1}$, where λ is a characteristic measure of the fluid relaxation time. The limiting viscosity value, corresponding to low shear rates, is called the zero shear rate viscosity, η_0 , and is defined by

$$\eta_0 = \lim_{\dot{\gamma} \rightarrow 0} [\eta(\dot{\gamma})] \quad (6)$$

The zero shear rate viscosity, η_0 , provides a measure of the fluid rheology under near-equilibrium conditions and is correlated to the molecular weight of the polymer through theory and calibration.¹⁶ The infinite shear rate viscosity, found at very high shear rates, is usually close to the solvent viscosity. The shear thinning region between the maximum and minimum viscosities typically exhibits a power law decrease in the viscosity with increasing rate.¹⁵ Graessley's entanglement theory attributes the non-Newtonian viscosity behavior to the effect of shear rate on entanglement density.¹⁸ As shear rate is increased, polymer chains become increasingly disentangled resulting in lower viscosities. The point of transition from the low shear rate plateau to the shear thinning region occurs at a critical shear rate, $\dot{\gamma}_{\text{crit}}$, which is of the order of the reciprocal of the relaxation time, λ . At low concentrations, the critical shear rate is roughly independent of concentration and scales as¹⁵

$$\dot{\gamma}_{\text{crit}} \sim 1/\beta \sim RT/[\eta]\eta_s M \quad (7)$$

where $[\eta]$ is intrinsic viscosity, defined from eq 1, η_s is the solvent viscosity, M is the molecular weight, R is the universal gas constant, and T is temperature. At higher concentrations, $\dot{\gamma}_{\text{crit}}$ correlates linearly with the product of concentration and viscosity-averaged molecular weight, M_v .¹⁵ Higher values of critical shear rate correlate with solutions of increased polydispersity.

The variation in the viscosity of a non-Newtonian fluid can be characterized by a number of simple models. For engineering work, the shear thinning region is often described by a power law expression of the form

$$\eta = m(\dot{\gamma})^{n-1} \quad (8)$$

where η is the solution viscosity, $\dot{\gamma}$ is the shear rate (in units of s^{-1}), m is a polymer specific constant (often called the consistency index) (with units of $\text{Pa}\cdot\text{s}^n$), and n is a dimensionless exponent specific to a particular polymer solution. For LPA dissolved in deionized water, these specific parameters have been experimentally calculated as 0.766 $\text{Pa}\cdot\text{s}^n$ and 0.326, respectively, for molecular weights greater than 10^5 .²⁷

Another model commonly used in rheology is the Carreau model.¹⁵ The Carreau model is a five-parameter model that incorporates the critical shear rate of the polymer in its calculation of solution viscosity, η .

$$\frac{\eta - \eta_s}{\eta_0 - \eta_s} = \frac{1}{[1 + (\lambda\dot{\gamma})^2]^{(1-n)/2}} \quad (9)$$

where η_0 represents the limiting viscosity at zero shear rate, η_s represents the solvent viscosity, $\lambda = (\dot{\gamma}_{\text{crit}})^{-1}$ is the critical shear rate for onset of shear thinning, and n is the exponent for the shear thinning region. In the present work, we regress our experimental measurements of $\eta(\dot{\gamma})$ to eq 9 and evaluate the degradation in the molecular weight in terms of the variation in η_0 and $\dot{\gamma}_{\text{crit}}$.

Effects of Shearing. Many equations that define and relate characteristic parameters of an entangled polymer network to specific properties of the polymer chains are only applicable for near-equilibrium conditions. As a result, equations that define network properties such as the distance between entanglement junctions, network chain length, and so on, neglect the effects of imposed shear. For instance, in concentrated solutions, the distance between two entanglement points is characterized by an average mesh size, ζ . A generalized formula for the mesh size of an entangled solution was proposed by Cottet et al.:²⁸

$$\zeta = 1.43 \left(\frac{k^{3/2}}{6} c^* \right)^{1/3a} \left(\frac{3}{4\pi N_A c} \right)^{((a+1)/3a)} \quad (10)$$

where k and a are the characteristic polymer–solvent parameters used in the Mark–Houwink–Sakurada equation, c^* is the critical concentration, c is the solution concentration, and N_A is Avogadro's number. This expression indicates that the mesh size of a polymer network is dependent only upon solution concentration and implies

that two entangled solutions with $M_w \gg M_c$ of the same polymer and concentration, have the same mesh size regardless of their molecular weights. However, the Cottet and Viovy equation was derived for highly entangled polymers in the unperturbed state. The shear-induced degradation effects on LPA solutions resulting from gel-loading and the semidilute entangled characteristics of the solutions make it inappropriate to rely upon such equations for nonequilibrium conditions.

Shear imposed on polymer strands can cause coil disentanglements or chain scission, both of which severely distort the matrix mesh size and number of entanglements, thus affecting DNA migration and separation. Electrophoretic studies of DNA separations using low molecular weight polymer solutions, or solutions that were not well entangled, reveal increased peak widths in the resulting electrophoregrams.^{4,8,9} Further, disentangled polymer strands allow electrophoretic motions of DNA within the matrix which would otherwise be restricted.⁹ Changes in the molecular structure of the sieving matrix can be detrimental to separations as evidenced by video microscopy studies^{6,7} which illustrate how DNA molecules actively drag surrounding polymer chains during electrophoresis. To resist such deformations, the matrix chains must be well-entangled. The referenced experiments highlight how shear-induced degradation of the polymer matrix during gel-loading may reduce the resolution and quality of separations.

Although shear imposed during gel-loading may result in temporary chain disentanglement, chain scission, or both, each effect will degrade the molecular weight and the entanglement density of the polymer solution. To quantify these effects, we define the percentage molecular degradation, D_p , for a sheared polymer solution. The quantity, D_p , refers to the shear-induced degradation of a polymer's viscosity-averaged molecular weight, M_v , during gel-loading and is defined as

$$D_p = \frac{M_v|^o - M_v|^f}{M_v|^o} \times 100\% \quad (11)$$

where $M_v|^o$ represents the viscosity-averaged molecular weight of the original polymer solution and $M_v|^f$ represents the final viscosity-averaged molecular weight of the polymer following shearing. Since viscosity scales with molecular weight to the 3.4 power,¹⁵ small changes in molecular weight translate into large changes in viscosity. By using the viscosity-averaged molecular weight, the effects of polymer chain disentanglements and chain scission can be seen by a decrease in the solution viscosity. Note, by its definition, the percent molecular degradation, D_p , will measure a reduction in the viscosity-averaged molecular weight of the polymer solution whether it is solely a result of chain disentanglement, chain scission, or a combination of both. To identify which effect is prevalent, additional techniques not incorporated in this study, such as light scattering or gel permeation chromatography (GPC), provide a more detailed analysis of the full molecular weight distribution.

Scaling arguments can be used to provide a more physical understanding of the quantity we have defined percent degradation, D_p . If one assumes the effects of shear-induced degradation lie solely in the lengths of the polymer strands, values of D_p can be correlated to these chain lengths. The weight average molecular weight of a polymer solution is defined as¹⁵

$$M_w = \sum (x_i M_i) M_i / \sum x_i M_i \quad (12)$$

where M_i is the molecular weight and x_i is the fraction of chains with molecular weight M_i . Models of entangled polymer solutions^{24,34} illustrate that molecular weight, M_i , is proportional to the chain contour length, L_i . Using this scaling, percent degradation, D_p , can be expressed in terms of the different polymer lengths, L_i , within the solution before and after shearing.

$$D_p = \frac{M_i^o - M_i^f}{M_i^o} \times 100\% = \frac{\sum (x_i L_i^2)^o - \sum (x_i L_i^2)^f}{\sum (x_i L_i^2)^o} \times 100\% \quad (13)$$

It is clear from eq 13 that percent degradation values do not scale directly with the lengths of the degraded chains. There is no linear relation because polymer chains are not always degraded nor must they always degrade to the same length. Thus, a 50% degradation value does not mean that all polymer chains are broken in half. In fact, using eq 13, a much higher average degradation value of 75% is obtained for such a case.

The effect of shearing in a capillary is further complicated by the fact that the flow is spatially nonhomogeneous. Solving the equations of motion reveals that the shear stress, τ , varies linearly from zero along the centerline to a maximum value at the wall.¹³ Since the shear-dependent viscosity of an entangled polymer solution is a strong function of the imposed deformation rate, the familiar parabolic velocity profile expected for a Newtonian fluid is also modified. By substituting an appropriate constitutive relation such as the power law of eq 8, the modified profile can be determined. For a shear thinning fluid, the shear rate is highest, and hence the viscosity is lowest, near the wall. The resulting velocity profile is "pluglike" with shearing effects confined to regions near the no-slip boundaries of the channel, i.e., the walls.

Using the power law constitutive model for a shear thinning fluid, an analytical expression for steady, fully developed flow through a circular channel can be obtained.¹⁵ In particular, the shear stress at the wall τ_w is found to be

$$\tau_w = \eta(\dot{\gamma}_w) [(Q/\pi R^3)(3 + 1/n)] \quad (14)$$

where $\eta(\dot{\gamma}_w)$ is the viscosity evaluated at the wall, $\dot{\gamma}_w$ is the shear rate at the wall, Q is the volume flow rate, R , the channel inner radius, and n is the exponent for the shear thinning region. The shear rate is largest at the wall and the ratio of the wall shear rate, $\dot{\gamma}_w$, to the average, $\langle \dot{\gamma} \rangle$, is

$$\frac{\dot{\gamma}_w}{\langle \dot{\gamma} \rangle} = \frac{\dot{\gamma}_w}{Q/\pi R^3} = (3 + 1/n) \quad (15)$$

as n decreases it is clear that the local shear rate near the wall becomes increasingly large. The analytical expression for shear stress indicates that values of shear rate at the wall, $\dot{\gamma}_w$, and shear stress at the wall, τ_w , during gel-loading are on the order of 10^2 – 10^3 s⁻¹ and 10^5 – 10^6 Pa, respectively. Note, previous work

indicates that even stresses less than 10^4 Pa result in the degradation of high molecular weight polymers.³¹

Electrophoretic Analysis. The performance of any electrophoretic procedure depends on the interband spacing and peak widths.³⁵ Selectivity is a measure of the relative difference in analyte mobility and is determined from the electrophoregram interband spacing. Resolution, R_L , is a measure of the separation capacity and is determined by the peak widths and spacing on the electrophoregram. It is defined as

$$R_L = 2 \sqrt{2 \ln 2} \frac{\Delta t_R}{(W_{h1} + W_{h2})} \quad (16)$$

where Δt_R is the difference in the retention time in seconds and W_{h1} and W_{h2} represent the peak widths at half-maximum between two successive peaks, also measured in seconds. The effects of any shear-induced degradation of LPA during gel-loading can be quantitatively measured from the loss in resolution between electrophoretic runs. As the molecular weight of a polymer solution is decreased due to shearing, the number of entanglements is also decreased, as is the length of the chains in the case of chain scission. Although these effects do not alter the solution pore size above the critical concentration, they do affect the sieving properties of the polymer. The result is wider peak widths during separations and subsequently lower resolution values.^{8,9}

MATERIALS AND METHODS

Synthesis and Calibration of LPA Separation Matrixes.

LPA powders (Poly Science Standards) of 1.1, 4.36, 8.78, and 12.1 MDa were slowly dissolved in deionized (DI) water to obtain 2 and 3% (w/v) solutions for gel-loading. The viscosity-averaged molecular weight, M_v , of each polymer sample at 25 °C was determined using an Ostwald viscometer. This device measures the intrinsic viscosity, $[\eta]$, of the sample which when combined with the Mark–Houwink–Sakurada equation¹⁵ yields the molecular weight. For LPA, the Mark–Houwink–Sakurada constant, k , is 0.006 31 mL/g and the dimensionless exponent, a , is 0.755.²⁷ The viscosity data of these solutions, η_0 , were then used to generate a separate molecular weight calibration curve for each concentration of LPA. Each curve was then fitted with a power law relation to facilitate calculations of percent degradation, D_p . Note, although LPA solutions of various molecular weights were used for calibration purposes, only LPA solutions with a viscosity-averaged molecular weight of 9×10^6 were used for degradation experiments.

For electrophoretic results, high-viscosity-averaged molecular weight LPA 9×10^6 powder was synthesized in-house according to the procedure described by Goetzinger et al.³⁶ LPA solutions were prepared using 1 × TBE (90 mM Tris/64.6 mM boric acid/2.5 mM EDTA) with 3.5 M urea/30% (v/v) formamide or with 1 × TTE (50 mM Tris/50 mM TAPS/2 mM EDTA) with 7 M urea. The solutions were ready for use after 3 days of slow stirring in a glass jar.

Micromachining. The design of the microdevice used for DNA separations and the laser-induced fluorescence (LIF) detec-

(34) deGennes, P. G. *Scaling Concepts in Polymer Physics*; Cornell Publishers: Ithaca, NY, 1989.

(35) Foret, F.; Krivankova L.; Bocek, P. *Capillary Zone Electrophoresis*; VCH Publishers: Weinheim, 1993.

(36) Goetzinger, W.; Kotler, L.; Carrilho, E.; Ruiz-Martinez, M. C.; Salas-Solano, O.; Karger, B. L. *Electrophoresis* **1998**, *19*, 242–248.

tion system have both been described previously.¹⁰ Electrophoretic microdevices were made from 150-mm-diameter glass wafers (Corning, Corning, NY) using techniques described in the literature.¹⁰ The device uses a cross injector for sample introduction with a hemispherical separation channel 11.5 cm in length, 40 μm deep, and 90 μm wide. The side channels forming the injector were 2.5 mm in length and horizontally offset by 250 μm . Glass reservoirs (Ace Glass, Vineland, NJ) of 50- μL volume were affixed around the channel access holes to hold the sample and buffer. Channel inner surfaces were coated with LPA using a modified Hjerten procedure.³⁷

Electrophoresis. Between each run, the separation and cross-injector channels of the device were simultaneously refilled with fresh LPA solutions from the anodic end of the separation channel using a gastight syringe. The electrophoresis buffer composed of 1 \times TTE was also changed after each run. Pre-electrophoresis was performed at 55 $^{\circ}\text{C}$ for 3 min at 200 V/cm. The DNA sequencing samples were loaded by applying a negative potential of 1500 V (300 V/cm) to the sample reservoir with the waste reservoir at ground and the buffers in both the anode and cathode reservoirs left floating. Leakage of excess sample from the loading procedure into the separation channel during the run was prevented with a small electric field (~ 20 V/cm) applied to both halves of the loading channel.

DNA Sequencing Reactions. DNA sequencing reactions were conducted using standard cycle sequencing chemistry with AmpliTaq-FS and BigDye-labeled M13 universal primers (Applied Biosystems/Perkin-Elmer Corp., Foster City, CA) and M13mp18 as template (New England Biolabs, Beverly, MA). A total of 0.4 μg of template DNA was used per sample (0.1 μg of M13mp18 per single-color reaction). Cycle sequencing was performed on a Genius thermocycler (Techne, Duxford, Cambridge, U.K.) consisting of 15 cycles of 10 s at 95 $^{\circ}\text{C}$, 5 s at 50 $^{\circ}\text{C}$, and 1 min at 70 $^{\circ}\text{C}$, followed by 15 cycles of 10 s at 95 $^{\circ}\text{C}$ and 1 min at 70 $^{\circ}\text{C}$.

Sequencing Sample Purification. The DNA sequencing samples were desalted using Centri-Sep spin columns (Princeton Separations, Adelphia, NJ). The spin columns were hydrated for at least 30 min by adding 800 μL of deionized water. The interstitial volume was excluded by spinning the columns for 3 min at 3000 rpm. The sequencing sample was diluted in 40 μL of deionized water and then placed in the column and spun for 3 min at 3000 rpm. The resulting sample volume was diluted to 50 μL with deionized water, and a 10- μL aliquot was then pipetted onto the electrophoretic device.

Data Analysis. The C-traces of four-color DNA sequencing reactions using ($\sim 21\text{M}13$) forward BigDye primers were used for data analysis. The C-traces were selected due to minimal crosstalk and ease of tracking single isolated peaks over the entire range of fragment sizes. From the resulting electrophoregrams, the migration time of the sequencing fragments versus base pair number were plotted and curved fitted with a third-order polynomial using Microcal Origin 6.0 software (Microcal Software Inc., Northampton, MA). The fitted values were used to calculate resolution as defined previously in eq 16.

Experimental Procedure. The apparatus shown in Figure 2 simulates a gel-loading protocol using automated pumping. The

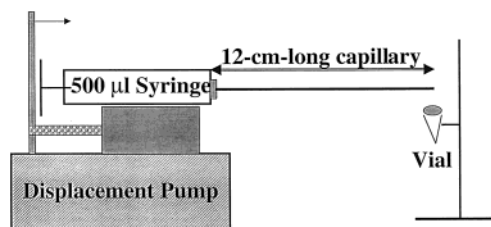


Figure 2. Schematic of experimental apparatus used to gather LPA solutions as they were loaded into electrophoretic channels at different flow rates.

apparatus consists of a syringe pump (Harvard Apparatus, Harvard, MA), a 500- μL gastight syringe (Hamilton, Reno, NV), uncoated fused-silica capillaries (Polymicro Technologies, Phoenix, AZ), stainless steel tees, ferrules, and plastic collection vials. LPA solutions of 2 and 3% (w/v), dissolved in deionized water and molecular weight 9×10^6 , were pumped through 12 cm of 50- μm and 75- μm -internal diameter (i.d.) capillaries at different fill rates and collected into plastic vials for viscosity testing.

To select appropriate volume flow rates, we estimated reasonable fill times for 12-cm-long channels. As mentioned earlier, these fill times were converted into volume flow rates using the microliters of LPA injected into each channel. Flow rates for this study ranged between 1 and 33 $\mu\text{L}/\text{min}$ corresponding to average wall shear rates, $\dot{\gamma}_w$, of 10^2 and 10^3 s^{-1} , respectively, as seen from eq 5. The flow rate of 1 $\mu\text{L}/\text{min}$ was the minimum rate attainable using automated pumping, while the maximum rate of 33 $\mu\text{L}/\text{min}$ was chosen as a worst case representation of manual gel-loading. Due to the large range of flow rates studied, throughout the remaining sections, the volume flow rate of 15 $\mu\text{L}/\text{min}$ is referred to as the “typical” or “average” rate during gel-loading.

The non-Newtonian viscosity profile of each collected polymer sample was analyzed using a commercial cone and plate rheometer (AR 1000-N, TA Instruments) with torques in the range 10–1000 $\mu\text{N}\cdot\text{m}$. To enable further study, the same LPA solutions were later used as sieving matrixes for DNA separations. For these later experiments, LPA solutions were loaded into microfabricated channels using the same apparatus and identical flow rates.

RESULTS AND ANALYSIS

Effects in Polymer Samples of 2 and 3% LPA. Figure 3 depicts the non-Newtonian viscosity profiles of an LPA solution after it has been pumped through a 12-cm-long capillary of 50- μm -i.d. at different flow rates. The solution shown is a 3% (w/v) LPA solution, dissolved in deionized water, with a molecular weight of 9×10^6 . The uppermost curve is the viscosity profile of the original LPA solution loaded at the lowest flow rate, while the remaining curves represent the profiles of each polymer sample loaded into the capillary at increasing flow rates. All data was gathered at 25 $^{\circ}\text{C}$ with less than 0.7 $^{\circ}\text{C}$ variation as measured by the rheometer. The measurements show that each curve retained the shape of the original viscosity profile but displayed much lower values of viscosity at every shear rate. It is also seen that the zero shear rate viscosity, η_0 , of each loaded polymer solution decreased as the fill rate was increased. If no molecular degradation were present, the viscosity profile of each polymer sample would be identical. Yet the behavior shown in Figure 3 indicates shear-induced degradation is present at every fill rate

(37) Hjerten, S. J. *J. Chromatogr.* **1985**, *347*, 191–198.

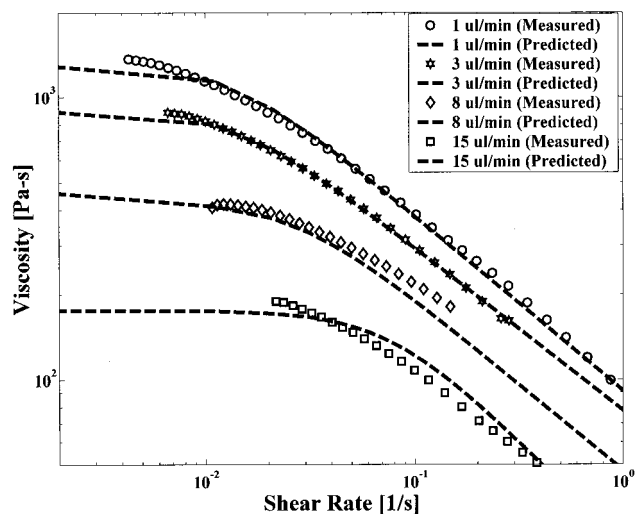


Figure 3. Non-Newtonian viscosity profiles of 3% (w/v) LPA solutions at 25 °C after gel-loading was performed within a 50- μ m-i.d. capillary at different volume flow rates. The polymer solution shown was dissolved in deionized water and of molecular weight 9×10^6 before gel-loading. The symbols represent viscosity data gathered using the rheometer while the dashed lines represent the viscosity predictions of the Carreau model for each flow rate.

during gel-loading. As seen from the definition of viscosity-averaged molecular weight, M_v , in eq 4, the measured decreases in viscosity indicate chain disentanglement, coil fracture, or combinations of both are present during gel-loading. Further, the lower values of viscosity corresponding to polymer samples loaded at higher flow rates indicate shearing effects increase with increased gel-loading rates. In such a sheared polymer solution, not only are the viscosity and average molecular weight decreased, but the strand length, pore size, and distribution functions of each are also affected.⁹ Changes in such parameters will generate substantial differences in the entanglement density and network pore size of the original sieving matrix, thereby influencing DNA migration within the LPA solution.

Via calibration, the zero shear rate viscosity, η_0 , of each polymer solution following gel-loading was used to determine the new viscosity-averaged molecular weight, M_v , of the shear-degraded polymer. Note, it is difficult to obtain viscosity data in the zero shear rate region because of the difficulty in obtaining shear rates below 10^{-2} s^{-1} experimentally for polymers. Further, the viscosity curves shown in the figure begin with different shear rates due to minimum torque constraints. The minimum obtainable torque, T_{\min} , for any experiment, using the commercial rheometer is $1 \mu\text{N}\cdot\text{m}$. Hence, as the zero shear rate viscosity of a polymer sample decreases, the minimum obtainable shear rate must increase to maintain the $0.1 \mu\text{N}\cdot\text{m}$ minimum torque criteria:

$$T_{\min} = [\tau_{\min}] \frac{2\pi R^3}{3} = [\eta(\dot{\gamma}_{\min}) \dot{\gamma}_{\min}] \frac{2\pi R^3}{3} \quad (17)$$

As a result, viscosity measurements of the samples with lower molecular weight begin with higher shear rates.

To ensure that the viscosity measured at the lowest attainable shear rate was representative of the zero shear rate viscosity, all

Table 1. Experimental Values of Zero Shear Rate Viscosity, η_0 , Viscosity-Averaged Molecular Weight, M_v , and Percent Degradation, D_p , for 2% (w/v) LPA Solutions^a

Q ($\mu\text{L}/\text{min}$)	η_0^{50} (Pa·s)	M_v^{50} ($\times 10^6$)	D_p^{50} (%)	η_0^{75} (Pa·s)	M_v^{75} ($\times 10^6$)	D_p^{75} (%)
3	129.4	8.41	4.16			
8	77.6	6.82	22.35	121.5	8.19	6.72
15	62.06	6.33	27.96	105.6	7.73	11.90
20	55.37	5.95	32.17	77.73	6.82	22.32
33	47.88	5.17	41.12	50.19	5.59	36.33

^a The samples, dissolved in deionized water with original molecular weights of 9×10^6 , were loaded into 50- and 75- μ m-i.d. capillaries at varying flow rates and 25 °C.

Table 2. Experimental Values of the Zero Shear Rate Viscosity, η_0 , Viscosity-Averaged Molecular Weight, M_v , and Percent Degradation, D_p , for 3% (w/v) LPA Solutions^a

Q ($\mu\text{L}/\text{min}$)	η_0^{50} (Pa·s)	M_v^{50} ($\times 10^6$)	D_p^{50} (%)	η_0^{75} (Pa·s)	M_v^{75} ($\times 10^6$)	D_p^{75} (%)
1	1370	8.66	1.31			
4	882.9	7.54	14.10	1342	8.61	1.94
8	455.3	6.12	30.35	1050	7.97	9.25
15	182.7	4.58	47.81	851.2	7.45	15.09

^a The samples, dissolved in deionized water with original molecular weights of 9×10^6 , were loaded into 50- and 75- μ m-i.d. capillaries at varying flow rates and 25 °C.

of the values of η_0 calculated experimentally were compared to those predicted by the Carreau model described in eq 9. The values of zero shear rate viscosity predicted by the model were within 8% of the η_0 values obtained experimentally using the rheometer. Thus, the viscosity data obtained experimentally for shear rates of order 10^{-2} s^{-1} were good estimates of the zero shear rate viscosity, η_0 . The Carreau model is curve-fitted to the experimental data in Figure 3 and is represented by dashed lines.

Rather than show the viscosity profiles of each experiment, Tables 1 and 2 summarize the parameters of interest to this study: zero shear rate viscosity, η_0 , viscosity-averaged molecular weight, M_v , and molecular degradation, D_p . Table 1 illustrates the changes in the molecular weight experienced by a 2% LPA solution when loaded into a 50- and 75- μ m-i.d. capillary at different flow rates. Using the 50- μ m capillary, the molecular weight of the polymer decreased by 4% when the solution was loaded at a flow rate of 3 $\mu\text{L}/\text{min}$, but decreased by 41% when loaded at the maximum rate of 33 $\mu\text{L}/\text{min}$. Similarly, in the 75- μ m capillary, a fill rate of 8 $\mu\text{L}/\text{min}$ resulted in a 7% decrease in molecular weight while a volume flow rate of 33 $\mu\text{L}/\text{min}$ produced a degradation of 36%. The average gel-loading rate of 15 $\mu\text{L}/\text{min}$ produced a 28% molecular weight degradation through the 50- μ m capillary, but only a 12% degradation when loaded in the larger 75- μ m capillary. From these data, it appears that the shear degradation experienced during gel-loading is larger in smaller diameter passages.

Table 2 summarizes the changes in molecular weight observed for a 3% (w/v) LPA solution loaded into a 50- and 75- μ m-i.d. capillary. The values of viscosity-averaged molecular weight, M_v , shown in Table 2 also illustrate lower levels of polymer degradation in the 75- than in the 50- μ m-i.d. capillary. During the average

15 $\mu\text{L}/\text{min}$ gel-loading, the 3% polymer solution experienced a 15% molecular weight degradation within the 75- μm capillary, compared to a 48% degradation within the smaller capillary. However, further comparison of the degradation values obtained with the 2 and 3% LPA solutions indicate shear-induced degradation is more sensitive to changes in concentration than to small variations in cross-sectional area. Previously, a 2% LPA solution loaded at a rate of 3 $\mu\text{L}/\text{min}$ within a 50- μm -i.d. capillary resulted in a 4% degradation. Using a 3% LPA solution, the decrease is a factor of 4 higher at 14%. In fact, when 3% solutions are used, even the lowest attainable flow rate of 1 $\mu\text{L}/\text{min}$ results in a 1% polymer degradation.

Note, as discussed earlier, since percent degradation is obtained from the calibration of viscosity-averaged molecular weight, M_v , degradation values do not correlate one to one with changes in polymer length. For example, Table 1 illustrates that the average gel-loading rate of 15 $\mu\text{L}/\text{min}$ through a 50- μm -i.d. capillary produced a 28% degradation in viscosity-averaged molecular weight. Using eq 13, this means that roughly 25% of the chains were broken in half during this gel-loading. Similarly, the 15% degradation experienced by the gel in the larger capillary indicates that $\sim 12\%$ of the chains were broken in half. Looking at Tables 1 and 2, values of percent degradation for solutions gel-loaded within a 50- μm capillary ranged from 4 to 47%, indicating roughly 3–48% of the polymer chains were broken in half. Solutions gel-loaded within the larger capillary experienced 1–36% degradation, indicating only 1–33% of polymer chains were broken in half.

The effects of chain disentanglement in these experiments can be monitored using viscoelastic stress relaxation measurements. The relaxation time of a polymer is a measure of its “fading memory” of previous deformations.¹⁵ For an entangled polymer solution, this stress relaxation arises principally by reptation, as the deformed polymer chains slowly diffuse along their confining “tube” until they regain their isotropic entangled configurations.³⁴ As mentioned in the Theory section, the critical shear rate, $\dot{\gamma}_{\text{crit}}$ is approximately the inverse of the polymer relaxation time, λ . The viscosity measurements shown here indicate that the relaxation time of the entangled LPA solutions used is on the order of 600–900 s. After two relaxation times, any residual memory of previous deformations, imposed during the loading process for example, will have decayed by a factor of e^{-2} and is thereby negligible.¹⁵ During the present experiments, as in practice, it was common to run electrophoretic separations 1 h after gel-loading. Given the polymer’s short relaxation time, coil disentanglement effects should be secondary when compared to the effects of coil scission.

Viscous Dissipation. Table 1, Table 2, and Figure 3 summarize the observed relationship and degradation between the viscosity of the LPA solutions and the volume flow rates at which they were loaded. In Figure 4 we compare the viscosity profiles obtained for each polymer sample and capillary at the average gel-loading rate of 15 $\mu\text{L}/\text{min}$. In the figure, higher LPA concentrations coupled with smaller cross-sectional areas produce the largest decrease in relaxation time and zero shear rate viscosity η_0 . The increased degradation can be attributed to the higher shear rates experienced by the more viscous fluid as it is loaded and displaced into smaller diameter passages. This is an important

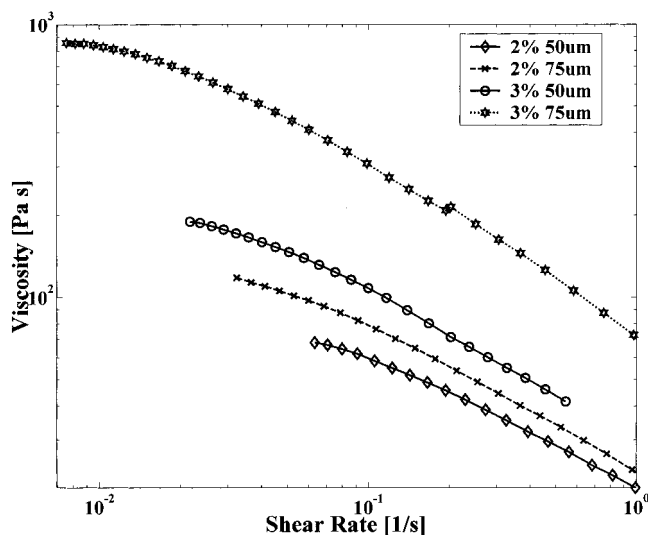


Figure 4. Non-Newtonian viscosity profiles of 2 and 3% (w/v) LPA solutions after gel-loading was performed at the average rate of 15 $\mu\text{L}/\text{min}$ in a 50- and 75- μm -i.d. capillary.

result for electrophoresis as many of the chemical additives commonly used as the buffered solvent for LPA solutions increase the viscosity of the sieving matrix, making the fluid more viscous and prone to degradation. Buffers that incorporate large amounts of urea, for example, generally increase the viscosity of the sieving matrix by 10% per 1 M urea added.¹⁷

As discussed earlier, the viscosity of a solution can be related to its molecular weight by eq 2. Due to the interpenetration of polymer chains in entangled solutions, increasing the polymer concentration will increase the solution viscosity nonlinearly.¹⁵ The higher entanglement density of polymer chains present in solutions of increased concentrations implies that the shear-induced degradation of polymeric solutions will increase with increasing viscosity.

An equation to estimate molecular degradation, D_p , based upon wall shear stresses, τ , and shear rates, $\dot{\gamma}$, imposed during gel-loading would greatly assist in selecting fill rates for any loading protocol. The rate of energy dissipated by the polymer in the form of chain scission and disentanglement is correlated with the product of the shear stress and shear rate, often called the viscous dissipation, Φ ,

$$\Phi = \tau : \dot{\gamma} \quad (18)$$

As defined in eq 18, viscous dissipation is a universal parameter that measures the rate of energy dissipation per unit volume in any system. It represents the external work that is irreversibly converted to thermal energy due to viscous effects in the fluid.¹³ To discuss viscous dissipation in the context of these experiments, the polymer is modeled as a power law fluid¹⁵ to obtain a more specific relation for Φ . Since both the shear stress and the shear rate vary nonlinearly in the channel, the local dissipation is integrated radially to obtain the expression

$$\Phi = \tau : \dot{\gamma} = m \left[\frac{Q(3 + 1/n)}{\pi R^3} \right]^{n+1} \quad (19)$$

where Q represents the volume flow rate during gel-loading (in

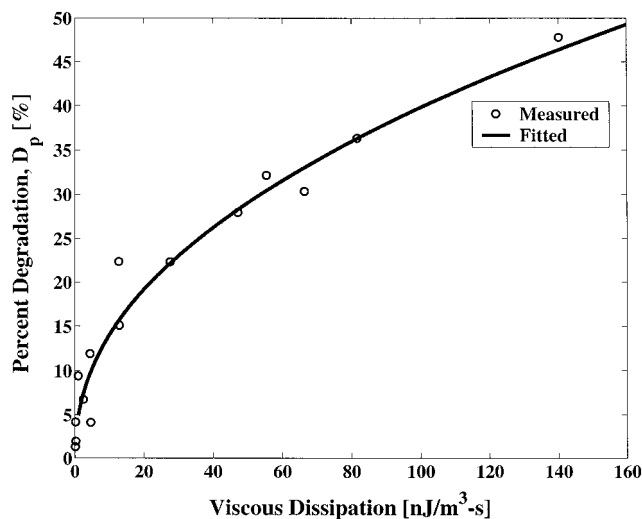


Figure 5. Experimental data of percent molecular degradation, D_p , plotted against the energy dissipated during gel-loading, Φ . The polynomial curve that fits the data is described by $D_p = 4.89\Phi^{0.445}$ with less than 7% error.

m^3/s), m is the consistency index of the polymeric solution (with units of $\text{Pa}\cdot\text{s}^n$), n is the dimensionless power law shear thinning exponent of the polymer, and R is the inner radius of the electrophoretic channel. The units of Φ as defined by eqs 18 and 19, correspond to energy density per second, or ($\text{J m}^{-3} \text{s}^{-1}$). Figure 5 displays the experimental data gathered for D_p plotted against the corresponding dissipation values described by eq 19. The data lie on a power law curve and can be used to estimate the molecular degradation expected for various gel-loading protocols. Using curve fitting, the data in Figure 5 can be described by the following equation with less than 8% error:

$$D_p = (4.89)\Phi^{0.445} \quad (20)$$

This equation shows that the percent degradation experienced by the polymer solution during gel-loading scales approximately as the square root of the power dissipated per unit time, or the square root of the viscous dissipation. Using eq 20, one can estimate the shear-induced degradation experienced by the polymeric solutions. For instance, when a 2% LPA solution was gel-loaded within a 75- μm capillary at the average flow rate of 15 $\mu\text{L}/\text{min}$, a 12% decrease in molecular weight was measured experimentally, as shown in Table 1. Using the equation in Figure 5 to estimate the degradation, one obtains a somewhat lower value of 10%. It should be noted that although viscous dissipation, Φ , is a universal parameter, its correlation with the derived parameter molecular degradation, D_p , is most valid for semidilute, entangled solutions of LPA. Additional experiments utilizing a larger concentration range are needed to quantitate the extent of shear-induced degradation of more concentrated solutions of LPA during gel-loading.

At first glance the estimated average gel-loading rate of 15 $\mu\text{L}/\text{min}$ might appear too conservative. However, for a 12-cm-long channel of 4418- μm^2 cross-sectional area (75- μm -i.d. capillary), the volume flow rate reveals that the channel volume is replaced 30 times/min during this gel-loading. Put into these terms, a 15 $\mu\text{L}/$

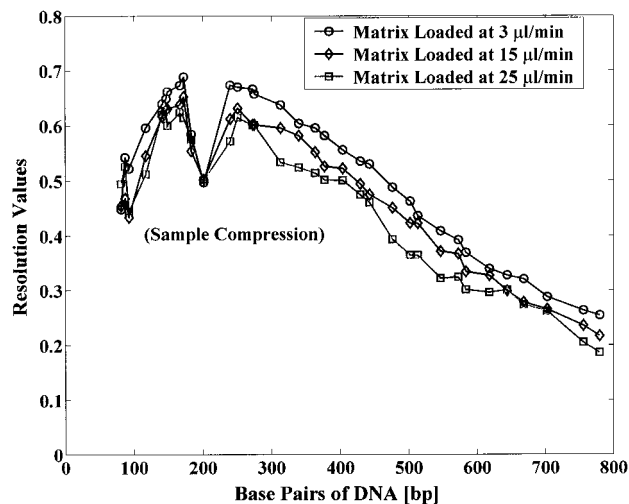


Figure 6. Resolution measurements obtained from electrophoregrams of DNA separations. The separations were performed with an LPA gel-loading of 3, 15, and 25 $\mu\text{L}/\text{min}$. Compression due to sample preparation protocol is noted.

min gel-loading is hardly conservative. By tripling the loading time to 3 min, the fill rate is reduced from 15 to 3 $\mu\text{L}/\text{min}$, and hence, the polymer volume is replaced only 6 times in 1 min. Since current experimental data indicate no polymer degradation is evident for such fill rates, the polymer degradation problem seems easily alleviated through implementation of longer gel-loading times.

Electrophoresis Measurements. Shear-induced degradation of LPA solutions during gel-loading has been clearly demonstrated through measurements of their viscometric properties. To observe how imposed shear influences DNA separations, each partially degraded polymer solution was used as a sieving matrix for DNA sequencing by microdevice electrophoresis. Experiments were reproduced over a 3-day period by two separate technicians. Microfabricated channels, 12 cm long and of 3600- μm^2 cross-sectional area, were loaded with 2% LPA solutions at carefully metered flow rates of 3, 15, and 25 $\mu\text{L}/\text{min}$ with the same apparatus described earlier. Note, the cross-sectional area of the microchannels was specifically fabricated to enable better comparison of the rheology data gathered in the circular 75- μm -i.d. capillary (4418- μm^2 area) to the electrophoretic results gathered in the rectangular microchannel (3600- μm^2 area).

Data analysis revealed broader peak widths and lower resolution values for faster loading rates. Each shear-degraded sieving matrix produced a resolution curve of the same shape but with decreasing resolution values as gel-loading rates were increased. From these experiments, it is seen that shear-induced degradation of LPA solutions does affect sequencing analysis as documented in Figure 6 and Table 3. Effects are most notable in the data showing the separation of DNA fragments larger than 300 bases.

Electrophoresis performed using the sieving matrix loaded at the lowest flow rate of 3 $\mu\text{L}/\text{min}$ produced separations that could resolve 380 base pairs of continuous DNA sequence with resolution values greater than 0.5, as defined by eq 16. Separations performed in the polymer loaded at the average rate of 15 $\mu\text{L}/\text{min}$ resulted in a lower read length of 323 bases, whereas the separations corresponding to the accelerated 25 $\mu\text{L}/\text{min}$ gel-loading were only able to resolve 283 bases. As indicated in Table

Table 3. Bases Resolved by Electrophoresis of an m13Mp18 DNA Cycle Sequencing Mixture on a 12-cm-Long Microfabricated Device^a

Q ($\mu\text{L}/\text{min}$)	continuous sequence with $0.5 R_L > 0.5$	no. of resolved bases
3	85–465	380
15	92–415	323
25	107–390	283

^a Separations were performed at 55 °C using 2% LPA solutions injected into electrophoretic channels at three separate flow rates as shown.

3, increasing the gel-loading rate from the average 15 to 25 $\mu\text{L}/\text{min}$ diminished read lengths by 12%. Conversely, a lower gel-loading rate of 3 $\mu\text{L}/\text{min}$ produced a 15% increase in the number of bases resolved over the average 15 $\mu\text{L}/\text{min}$ gel-loading and a 25% increase compared to the read lengths obtained using a 25 $\mu\text{L}/\text{min}$ gel-loading.

Admittedly, the significance of a 15% increase in the number of bases resolved may vary with the opinion of the researcher. However, the impact of such an improvement strongly depends on the application. For instance, when working with short tandem repeats (STRs), a 15% increase in the number of bases resolved can be the determining factor in DNA forensics.¹⁰ Further, when working with high-throughput screening devices such as those

in a genome center, a 15% increase in the number of bases resolved is rather substantial.

CONCLUSIONS

The data presented here illustrate how shear-induced degradation of the sieving matrix can result from improper gel-loading. Further, diminished resolution of subsequent DNA sequencing can be directly linked to this degradation. The experimental data also indicate degradation of the sieving matrix during gel-loading is more affected by the viscosity and concentration of the polymer than it is by the channel cross section. This implies that electrophoretic separations using more entangled solutions of LPA will sustain higher degradation than shown here. For LPA concentrations lower than 3% (w/v), induced degradation can be eliminated if the polymer is loaded at rates below 3 $\mu\text{L}/\text{min}$. Note, in all experiments, the most significant effects were seen in the separation of fragment sizes larger than 300 bases.

ACKNOWLEDGMENT

This work was supported by the National Institute of Health (NIH) under Grant HG01389 and by the Defense Advanced Research Projects Agency.

Received for review November 2, 2000. Accepted March 20, 2001.

AC001294+